AIAA JOURNAL
Vol. 37, No. 9, September 1999

Oscillatory Control of Separation at High Reynolds Numbers

A. Seifert* and L. G. Pack†
NASA Langley Research Center, Hampton, Virginia 23681

An experiment conducted in a pressurized, cryogenic wind tunnel demonstrates that unsteady flow control using oscillatory blowing (with essentially zero mass flux) can effectively delay flow separation and reattach separated flow on an airfoil at chord Reynolds numbers as high as 38×10^6. Oscillatory blowing at frequencies that generate one to three vortices over the controlled region at all times are effective over the entire Reynolds number range, in accordance with previous low-Reynolds-number tests. Stall is delayed and poststall characteristics are improved when oscillatory blowing is applied from the leading-edge region of the airfoil, whereas flap effectiveness is increased when control is applied at the flap shoulder. Similar gains in airfoil performance require steady blowing with a momentum coefficient that is two orders of magnitude greater. A detailed experimental and theoretical investigation was undertaken to characterize the oscillatory blowing disturbance, in the absence of external flow, and to estimate the oscillatory blowing momentum coefficient used in the cryogenic wind tunnel experiment. Possible approaches toward closed-loop active separation control are also presented. Based on the findings of the present investigation, the application of active separation control at incompressible flight Reynolds number is within reach.

Nomenclature

C_d = airfoil total drag coefficient
C_{dp} = airfoil pressure drag coefficient
C_l = airfoil lift coefficient
$C_{l,\max}$ = maximum lift coefficient
C_m = airfoil moment coefficient
C_p = pressure coefficient, $\equiv (P - P_S)/q$
C_μ = combined blowing momentum coefficient, $\equiv (c_\mu; \langle c_\mu \rangle)$
$\langle c_\mu \rangle$ = oscillatory blowing momentum coefficient, $\equiv \langle J' \rangle / cq$
c = airfoil chord
c_μ = steady blowing momentum coefficient, $\equiv J/cq$
F^+ = reduced frequency, $\equiv (f x_{te})/U_\infty$
f = oscillation frequency, Hz
h = slot height or width
J = momentum at slot exit, $\equiv \rho h U_j^2$
P = pressure
q = freestream dynamic pressure, $\equiv 1/2 \rho U_\infty^2$
R_c = chord Reynolds number, $\equiv U_\infty c/\nu$
T = temperature
U, u = average and fluctuating velocity
X/c = normalized streamwise location
X_{te} = distance from actuator to trailing edge
Y = distance normal to wall
Z = spanwise location
α = airfoil angle of attack
δ_f = flap deflection angle
ν = kinematic viscosity
ρ = density
$\langle \rangle$ = phase locked values

Subscripts

Avg = averaged
amb = ambient conditions
b = airfoil baseline parameters
cryo = cryogenic conditions
d = derectified hot-wire data
e = conditions at airfoil cavity exhaust
I = conditions at airfoil cavity inlet
j = conditions at blowing slot
s = tunnel static conditions
std = steady
t = tunnel total conditions
u = uncorrected airfoil parameters
∞ = freestream condition

Superscript

$'$ = root mean square of fluctuating value

I. Introduction

EXPERIMENTS performed at low Reynolds and Mach numbers[1–9] have shown that cyclic vortical oscillations introduced into a separating boundary layer slightly upstream of the average separation location can effectively delay boundary-layer separation. The improved ability of the boundary layer to overcome an adverse pressure gradient is attributed to enhanced mixing between the low momentum fluid near the wall and the external high momentum flow (similar to the plane, turbulent mixing layer[10]). This process becomes extremely efficient if the excitation frequencies correspond to the most unstable frequencies of the separating (almost free) shear layer, generating arrays of spanwise vortices that are convected downstream and continue to mix across the shear layer downstream of the excitation device. It was demonstrated[9] that the most effective frequencies for increasing the lift are $F^+ \approx 1$, for a range of low R_c.

Earlier attempts to control boundary-layer separation from airfoils used external sound source to excite the separating, laminar boundary layer.[11] The effective frequencies were very high ($F^+ = 14$–90), indicating that the excitation actually promoted transition. Transition is known to delay laminar separation because of the enhanced turbulent mixing. Later experiments[4] showed that sound emanating from holes in the surface is significantly more effective than external acoustic excitation. The effective frequencies of the internal excitation were $F^+ \approx 1.4$ (Ref. 4). Internal installation of a speaker was used to generate velocity perturbations at an excitation slot,[12] to promote flow reattachment of a separated shear layer. Drag and length of separated region were optimally reduced when using $F^+ \approx 2$ (based on the length of the baseline separated region[12]). The level of velocity perturbations at the slot exit, rather than the sound pressure level, served as an amplitude indication.[12] A clear demonstration that the control parameter is the excitation fluctuating

Presented as Paper 98-0214 at the AIAA 36th Aerospace Sciences Meeting, Reno, NV, 12–15 January 1998; received 2 March 1998; revision received 17 August 1998; accepted for publication 3 February 1999.

*NRC Research Associate; on leave from Department of Fluid Mechanics and Heat Transfer, Faculty of Engineering, Tel-Aviv University, 69978 Ramat-Aviv, Israel. Member AIAA.
†Research Engineer, Flow Modeling and Control Branch.

momentum, and not the sound pressure level, was provided later.[5] A vibrating wire[3] was also used to excite the flow upstream of the leading edge of a stalled airfoil. Mild benefits were observed, partly because of the limited capability of the wire, oscillating in a uniform flow, to generate vortical excitation. The optimal F^+ was 1.8 (Ref. 3). A vibrating device, operating inside the boundary layer, slightly upstream of the separation location, is more effective[2] because it mixes across the boundary layer, a source of steady vorticity. Enhanced aerodynamic loading at increased dynamic pressures, reliability, and durability issues limit the use of surface-mounted vibrating elements. Alternating blowing and suction through a surface slot allows the active element to be installed inside a cavity, protected from the external environment and well controlled. Selection of operational actuators would be determined by their capability to generate the required periodic excitation, efficiently, at low initial cost and with minimum maintenance and weight. Furthermore, the nature of the device used to generate the unsteady disturbances is not important as long as the vortical disturbances injected at the separation location are similar.[8] One way to generate cyclic vortical oscillations is by oscillatory blowing (alternating suction/blowing through a downstream directed slot[6]). This technique is very efficient because at the suction part of the cycle the low momentum fluid is sucked into the device, whereas in the blowing part of the cycle a high momentum wall-jet is superimposed on the separating velocity profile. In both cases the spanwise vorticity is enhanced. Oscillatory blowing allows independent control of the excitation magnitude, the frequency, and the average mass flux, whereas the airfoil geometry is almost unchanged by the presence of the narrow blowing slot. A detailed experimental and theoretical characterization of the oscillatory blowing disturbance was performed to evaluate the excitation used in the cryogenic wind tunnel experiment, where such measurement is impractical.

The delay of boundary-layer separation increases the airfoil maximum lift while maintaining low drag. When applied over deflected flaps, oscillatory blowing increases flap efficiency by delaying the flow separation from the flap upper surface, increasing the circulation around the entire airfoil. Oscillatory blowing is significantly more effective than steady, tangential blowing for separation control[6,9,13,14] because the steady wall-jet utilizes added momentum alone to overcome the adverse pressure gradient.

It has been hypothesized that unsteady separation control, especially with laminar separation, is similar to active boundary-layer tripping because both methods take advantage of an instability mechanism. To eliminate this hypothesis, transition strips were located at the leading edge (LE) region of airfoils and generic flap configurations.[7] It was shown that neither forced transition, thickened turbulent boundary layers, nor elevated Reynolds numbers (up to 3.3×10^6 tested previously[15]) had an adverse effect on the efficiency of the method. Moreover, as the R_c increases, the tendency of the boundary layer to separate decreases because of the increase of inertia relative to viscous forces (expressed also in the relative decrease between the momentum thickness at the separation location and the airfoil chord). Still a high-Reynolds-number demonstration was missing. The main purpose of the present investigation was to increase the range of R_c tested and to demonstrate the effectiveness of oscillatory blowing for separation control at high R_c, given the successful application at low R_c.

II. Experimental Setup

A. Overview

The experiment was conducted in a pressurized cryogenic wind tunnel, which has advantages and disadvantages for demonstration of active flow control. For example, a cryogenic pressurized facility allows independent control of R_c and M at a fixed freestream velocity. With this type of control, the effective frequencies are clearly indicated because F^+ can be held fixed when R_c is varied and M is held constant. Another advantage of testing in a cryogenic pressurized facility is the ability to generate a zero-mass-flux disturbance when using a pulsed injection valve. It was possible to exhaust all of the mass flux introduced by the oscillatory valve simply by venting the airfoil cavity, using the pressure difference between the wind tunnel and the exhaust side of the airfoil. On the other hand, one of the disadvantages of testing in a cryogenic pressurized facility is that an in situ determination of $\langle c_\mu \rangle$ is very difficult. However, using atmospheric bench-top tests and a simplified flow model, it is possible to estimate the $\langle c_\mu \rangle$ used.[13]

B. The 0.3-m Transonic Cryogenic Wind Tunnel

The experiment was conducted in the 0.3-m Transonic Cryogenic Tunnel at the NASA Langley Research Center. It is a closed-loop, fan-driven tunnel with a test cross section of 0.33×0.33 m. Gaseous nitrogen (GN_2) is the test medium. The tunnel operates at stagnation pressures ranging from 1.2 bar up to 6 bar and total temperatures from 78 K up to 327 K (Ref. 16). The floor and ceiling of the tunnel were diverged in the vicinity of the airfoil to reduce blockage resulting from boundary-layer growth on the test section walls. A survey rod extends from the left tunnel sidewall to traverse the airfoil wake vertically (Fig. 1). The wake rake was located 2.2 chords downstream from the airfoil mid-chord, the farthest downstream position available.[17]

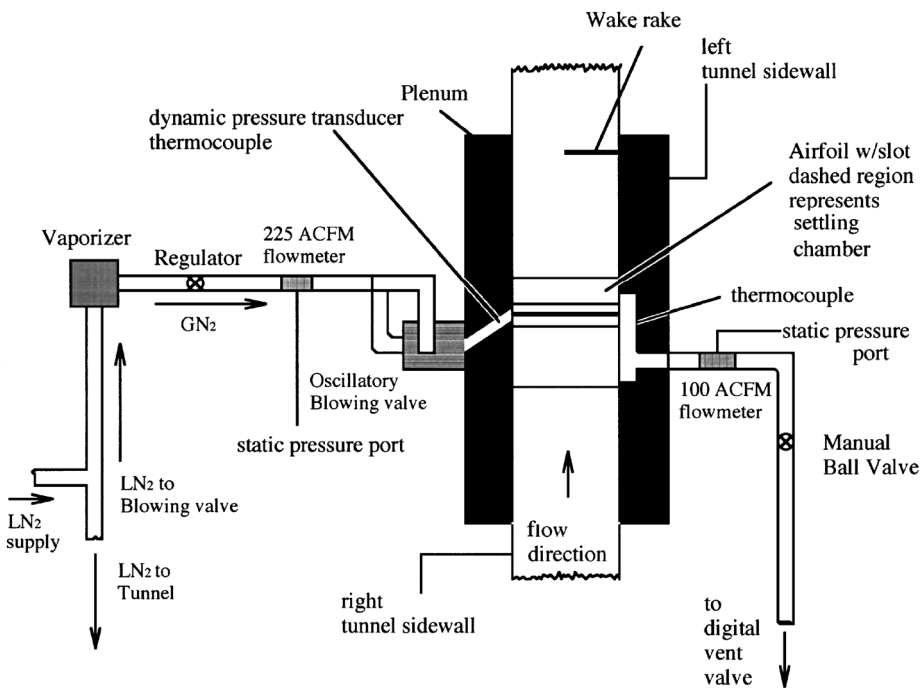

Fig. 1 A schematic description of the experimental setup in the 0.3-m Transonic Cryogenic Tunnel (top view).

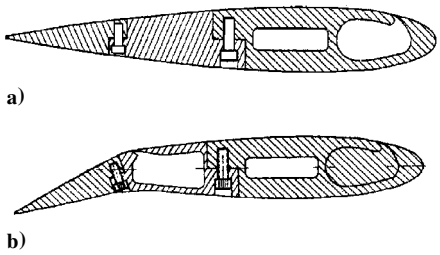

Fig. 2 NACA 0015 airfoil with a) a blowing slot at $X/c = 10\%$, b) a 30% TE flap deflected 20 deg and a blowing slot at $X/c = 70\%$. The LE cavity is sealed and filled with foam.

C. NACA 0015 Airfoil

Two variants of a 254-mm chord NACA 0015 airfoil were tested. In the first configuration (Fig. 2a), the airfoil was equipped with a blowing slot located on the upper surface at 10% chord, suitable for the control of separation near the leading edge, and in the second configuration (Fig. 2b), the airfoil was equipped with a 30% chord trailing-edge flap deflected 20 deg and a blowing slot located at 70% chord. In the latter case, the flow separates at the flap shoulder over a wide range of α and R_c. Both slots were about 0.2% chord wide (0.50 and 0.44 mm for the forward and rear slots, respectively), and allowed an almost tangential downstream introduction of excitation (the slots are inclined at 30 deg to the surface because of manufacturing considerations). When using the aft slot and cavity, the leading-edge cavity was filled with acoustic absorbing foam to eliminate cavity resonance and the sides of the cavity were sealed to eliminate the possibility of mass transfer.

D. Oscillatory Blowing System

A rotating, siren-type valve was used to generate the pressure oscillations inside the airfoil cavity. The oscillatory blowing valve was capable of operating at frequencies up to 600 Hz and for safety reasons was rated to 300 psi. GN_2 was supplied to the valve by converting a portion of the LN_2 (liquid nitrogen) available for operating the tunnel using an ambient temperature vaporizer. The use of ambient temperature GN_2 simplified the valve design. A pressure regulator was used to control the GN_2 entering the valve and the variable speed drive of the valve motor was used to control the frequency of the pressure oscillations. The oscillatory blowing valve was attached to the right tunnel plenum door at the center of rotation of the turntable (Fig. 1). A 49-mm-i.d. pipe was used to connect the valve to either the leading edge or the flap shoulder cavity. The exhaust side of the airfoil was connected to the tunnel boundary-layer removal system. The valves in the boundary-layer removal system were used to control the flow rate out the exhaust side of the airfoil cavity (Fig. 1). Any relevant combination of steady and oscillatory blowing could be generated with this type of control. Steady suction and blowing could be applied in a similar manner by holding the oscillatory blowing valve in the fully open position and varying the inlet and exhaust mass flow rates.

E. Instrumentation

Airfoil surface pressures were measured at 50 locations by the facility data acquisition system. Lift, moment, and form-drag were calculated from these measurements. Turbine flow meters on the inlet and exhaust sides of the model were used to measure the flow volume entering and exiting the airfoil cavity. The volume flow rate measurements were combined with temperature and pressure measurements to determine the mass flux entering and exiting the airfoil cavity. The steady mass flux in or out of the slot could be determined by subtracting the two mass fluxes. A dynamic pressure transducer, flush-mounted in the inlet pipe close to the airfoil cavity, was used to measure the pressure fluctuations produced by the oscillatory blowing valve.

F. Bench-Top Experiments

The velocity fluctuations exiting the slots of the airfoil were measured with the airfoil outside the tunnel using a hot-wire mounted on a three-dimensional traverse system. The GN_2 supplied to the oscillatory blowing valve during the wind tunnel test was replaced with compressed air. All of the pipe accessories were identical in both the wind tunnel and the bench-top experiments to maintain similarity between the two experiments. Although any desired combination of oscillatory and steady flow rates were obtainable in the cryogenic wind tunnel experiment, steady suction could not be applied in the bench-top experiments because of the atmospheric test conditions. However, even in the bench-top experiments, reverse flow in the slot was encountered because of the instantaneous, subatmospheric pressures created by the inertia of the continuous flow along the airfoil cavity. To better simulate the zero-mass-flux disturbance, a suction fan was connected to the exhaust pipe in some tests. The signals from the dynamic pressure transducer and the hot-wire were acquired using a 16-bit high-speed A/D, coupled with an anti-aliasing filter. In the cases where reverse flow was expected at the slot exit, the hot-wire signal was derectified to account for the reverse flow. Figure 3a presents the hot-wire data and Fig. 3b presents the simultaneously measured dynamic pressure data. The signals were first ensemble averaged over hundreds of periods of the pressure oscillations, which are used for phase reference. Figure 3a shows that the ensemble-averaged hot-wire data are similar to the raw hot-wire signal, indicating that the velocity signal at the slot exit contains very little random motion. To account for hot-wire rectification, the sign of the velocity signal was changed on the portion of the cycle with reverse flow present (as identified by the numerical scheme), whereas velocities close to zero (and outside the calibration range) were interpolated using neighboring points with valid velocities.

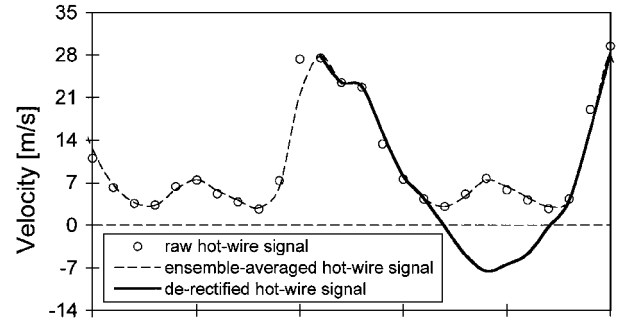

a) Raw, ensemble-averaged and derectified hot-wire signals

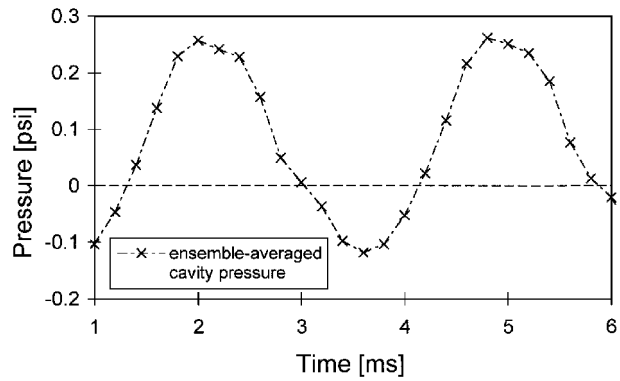

b) Corresponding cavity pressure fluctuations

Fig. 3 Hot-wire derectification process.

G. Experimental Uncertainty

Most of the experiments were conducted at conditions close to the limits of the wind tunnel operating envelope. For example, the very low temperatures (about 100 K) and Mach numbers (0.3 for the straight airfoil and 0.2 for the flapped airfoil) are close to the lower limit of the tunnel capability.[16] Most of the baseline data were acquired with separated flow regions present on parts of the airfoil. An additional source for error was the unsteadiness of the LN_2 pressure supplied to the tunnel and blowing system. Table 1 contains the relevant information regarding experimental uncertainties. These values were calculated using ± 3 standard deviations of the various experimental conditions and calculated parameters (including repeated

Table 1 Uncertainty of flow and control parameters

Item	Uncertainty, % full scale	Full scale and condition
LN_2 line pressure	3	150 psi
Slot width	5	0.02″ (0.5 mm)
Static temperature	0.3	300 K
Static pressure	0.5	22 psi and $M = 0.2$
Static pressure	2.4	77 psi and $M = 0.2$
R_c	2.5	$8–28 \times 10^6$ and $M = 0.2$
R_c	1	$11–38 \times 10^6$ and $M = 0.3$
M	2	$M = 0.2$
M	1.3	$M = 0.2$
F^+	6	2
c_μ	5	Local values
$\langle c_\mu \rangle$	30	Local values
f	0.1	600 Hz
U hot-wire	1.5	Local values
u'_d	15	Local values
p'	0.5	10 psi
x, y, z	0.01 mm	
T	0.2°C	

Table 2 Uncertainty of aerodynamic parameters

Parameter	Fully attached	Stalled	Controlled
C_{lu}	0.01	0.03	0.015
C_{dpu}	0.001	0.003	0.0015
C_{du}	0.001	0.003	0.002

runs). All of the specific instruments were calibrated prior to use. The uncertainty of the calculated airfoil aerodynamic parameters is listed in Table 2 (in absolute values and related to flow condition on the airfoil).

H. Experimental Conditions

Most of the experiments were conducted at a Mach number of 0.2 and chord Reynolds numbers ranging from 8.0×10^6 to 28.2×10^6 using the deflected flap configuration. Data were also acquired at $R_c = 37.6 \times 10^6$ and $M = 0.3$ using the $X/c = 10\%$ slot to study the improvement of poststall characteristics at the maximum available R_c.

III. Characterization of the Oscillatory Blowing for Cryogenic Testing

A. Overview

The following section establishes the theoretical background and assumptions that enable characterization of the oscillatory blowing in cryogenic conditions. The oscillatory blowing at the slot exit was generated by the unsteady pressure gradient imposed over the slot connecting the airfoil cavity and the external flow (Figs. 2a and 2b). The cavity pressure fluctuations were measured both in the wind tunnel and in bench-top tests. Specific correlations between $u_j'^2$ and p_I'/ρ_j (derived from the bench-top tests for all of the test frequencies) were used to estimate the $\langle c_\mu \rangle$ in the cryogenic conditions.[13]

The effect of replacing the GN_2 with air in the bench-top tests and real gas effects in the cryogenic conditions were neglected in light of the other, greater sources of uncertainty. The following analysis should not be considered as more than scaling arguments. It certainly does not attempt to present a solution for a specific flow situation at a given set of boundary conditions.

B. Model Flow

To model the flow through the slot connecting the airfoil cavity and the external flow simply (yet meaningfully), we considered flow through a two-dimensional channel, h wide and $5h$ long. The parallel Navier–Stokes equation describing this flow is

$$\frac{\partial u}{\partial t} + u\frac{\partial u}{\partial x} = -\frac{1}{\rho}\frac{\partial P}{\partial x} + \nu\frac{\partial^2 u}{\partial y^2} \tag{1}$$

where x is measured along the slot from its entrance and y is measured across the slot, with the boundary conditions

$$P(X = 0) = P_I + \sqrt{2}p' \sin(\omega t) \tag{2a}$$

$$P(X = 5h) = P_s = P_I \tag{2b}$$

This analogy neglects the effects of flow convergence at the high pressure side of the slot (which changes every half cycle in the case of a zero-mass-flux disturbance) as well as the geometrical slot convergence on the cavity side. This assumption could be justified because the density fluctuations are not neglected in the two-dimensional continuity equation, which takes the form

$$\frac{\partial \rho}{\partial t} \approx \frac{\partial(\rho u)}{\partial x} \tag{3}$$

allowing us to neglect the cross-stream derivative. At the low pressure side the flow can reasonably be approximated by a jet, which is almost parallel.

C. Scaling Arguments

In the following section we use order-of-magnitude considerations to derive the relationship between u' and p'. Because the fluctuating pressure gradient along the slot is

$$\frac{\partial P}{\partial x} = -\frac{\sqrt{2}p'}{5h}\sin(\omega t) \tag{4}$$

where it is assumed that the velocity along the slot is in the form

$$U(t, x, y) = u'(x, y)\sin(\omega t + \varphi) \tag{5}$$

and that the phase shift (φ) does not depend on x, the orders of magnitude of the various terms (neglecting viscosity[13]) in Eq. (1) become

$$\frac{\partial u}{\partial t} \propto \omega u' \cos(\omega t + \varphi) = \mathcal{O}(\omega u') \tag{6a}$$

$$\frac{1}{\rho}\frac{\partial P}{\partial x} \propto \frac{p'}{\rho h}\sin(\omega t) = \mathcal{O}\left(\frac{p'}{\rho h}\right) \tag{6b}$$

$$u\frac{\partial u}{\partial x} \propto u' \sin(\omega t + \varphi)\frac{\partial u'}{\partial x}\sin(\omega t + \varphi) = \mathcal{O}\left(\frac{u'^2}{h}\right) \tag{6c}$$

The scaling arguments for factors affecting the velocity fluctuation out of the slot as a function of the cavity pressure fluctuations are obtained by introducing Eqs. (6a–6c) into Eq. (1) to obtain

$$u'^2/h \propto p'/\rho h - \omega u' \tag{7}$$

Considering the relative magnitude of these terms at our experimental conditions, the leading relationship for low amplitudes is

$$u' \propto p'/\rho \tag{8}$$

whereas for large amplitudes it is

$$u' \propto \sqrt{p'/\rho} \tag{9}$$

This relationship will enable us to correlate the measured u', p', and ρ in the ambient bench-top tests, with the measured p'/ρ in the cryogenic conditions, and deduce from that correlation an estimation for u' at the slot exit under cryogenic conditions.

To test the existence of two amplitude regimes, the derectified slot velocity fluctuations u'_d are plotted against the fluctuating pressures at the entrance of the airfoil cavity (Fig. 4), for all of the frequencies and input pressure levels used in the bench-top experiment. These experiments were performed by fixing the static pressure at the entrance to the oscillatory blowing valve, scanning the entire frequency range, and simultaneously measuring the cavity fluctuating pressure and the slot exit velocity. The two amplitude regions are clearly shown, separated at $u'_d \approx 10$ m/s (Fig. 4). The appropriate slope (obtained by least-squares fit) for the low-amplitude region is about twice as high as the slope obtained for the large u'_d range, implying that, if u'_d is proportional to p'/ρ in the low-pressure range,

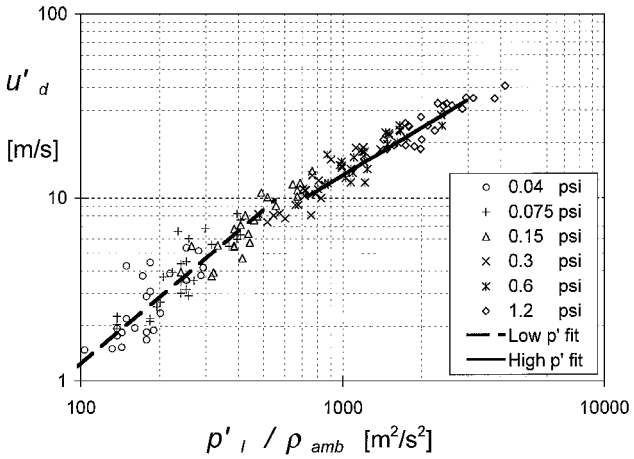

Fig. 4 Derectified slot exit velocity vs cavity pressure fluctuations, showing different slopes for the low- and high-amplitude ranges. Static pressures at the entrance to the oscillatory blowing valve are indicated in the legend.

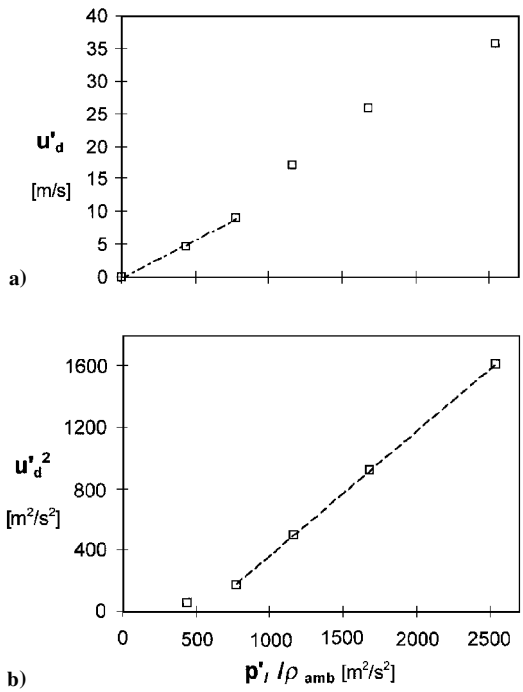

Fig. 5 Dependence of the slot velocity fluctuations on the cavity pressure fluctuations showing linear trends for the two amplitude ranges: a) u'_d is proportional to the cavity pressure fluctuations in the low-amplitude range, and b) u'^2_d is proportional to p' in the high-amplitude range.

then u'_d should be proportional to $\sqrt{(p'/\rho)}$ in the high-pressure range. The theoretical prediction for the power law relationships is further validated by examining the detailed calibration data for a frequency of 350 Hz, which was the most commonly used in the wind tunnel tests (Fig. 5). These u'_d values were obtained by averaging the data presented in Fig. 6, over the core region of the oscillatory jet. Figure 5a clearly shows the linear dependence between u'_d and p'_I/ρ_{amb} for the low-amplitude range, whereas Fig. 5b shows the linear dependence between u'^2_d and p'_I/ρ_{amb} for the high-amplitude range. Note that the same data are plotted in Figs. 5a and 5b.

D. Definition of the C_μ in the Cryogenic Conditions

The oscillatory blowing momentum coefficient is the relevant parameter to quantify the excitation introduced by the active device into the boundary layer. It was shown[8] that one obtains essentially the same flow characteristics when using different excitation mechanisms (i.e., vibrating ribbon and slot oscillatory blowing) when the

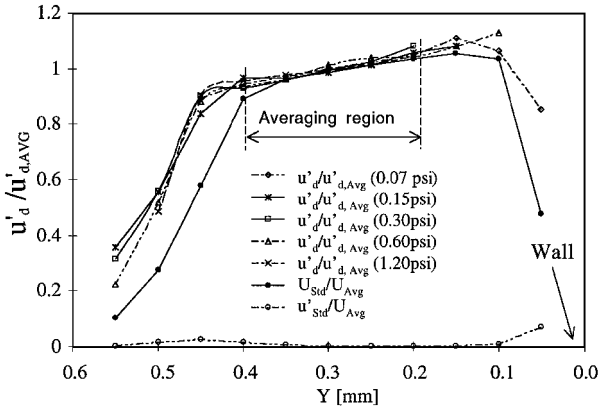

Fig. 6 Steady (Std) and oscillatory wall-jet velocity profiles, normalized (by U_{Avg} or $u'_{d,\text{Avg}}$) for a range of static pressures applied at the entrance to the oscillatory blowing valve ($f = 350$ Hz, $Z = 165$ mm).

oscillating momentum is integrated across the entire boundary layer close to the device or at the slot exit. The definition of the oscillatory blowing momentum coefficient is

$$\langle c_\mu \rangle \equiv \langle J' \rangle / cq \tag{10}$$

The J' should be calculated from u'_d measured at the slot exit in the absence of external flow. This is desirable because the unsteady jet significantly changes within a few slot widths even without external flow. Moreover, with external flow, the interaction between the disturbance and the external flow is dominated by the local pressure gradient, the characteristics of the upstream boundary layer, and the jet/external flow momentum ratios. Clearly there is not a single point in space in which the disturbance can be accurately and repeatedly characterized other than the slot exit.

Because of safety considerations, the GN_2 injected through the oscillatory blowing valve in the cryogenic wind tunnel experiment was at ambient temperature (above 225 K). When a zero-mass-flux disturbance was used, the blowing part of the disturbance was warm GN_2, whereas the suction part was cold GN_2 (because the tunnel was typically at 100 K). To account for this effect, one needs to calculate separately the momentum flux during the suction and blowing periods of the cycle (assuming a sine wave in time and a uniform velocity profile at the slot exit) to get

$$\langle J' \rangle = \frac{h(\rho_j + \rho_\infty)\langle u' \rangle^2}{2} \tag{11}$$

This will allow us to rewrite

$$\langle c_\mu \rangle \equiv \frac{h(\rho_j + \rho_\infty)\langle u' \rangle^2}{2cq} \tag{12}$$

Assuming further that the static pressure in the airfoil cavity is equal to the local static pressure on the airfoil at the slot location, and using the ideal gas relation

$$\rho = P/RT \tag{13}$$

we obtain

$$\langle c_\mu \rangle \equiv \frac{h}{c}\left(\frac{T_\infty}{T_j} + 1\right)\frac{\langle u' \rangle^2}{U_\infty^2} \tag{14}$$

For a temperature ratio of 1, this definition coincides with our ambient definition[7,9] of $\langle c_\mu \rangle$, but it decreases by 33% for the extreme case of a 1:3 temperature ratio, experienced at cryogenic conditions. When steady blowing was added to the oscillatory blowing, such that the flow was always out of the slot, the oscillatory and the steady momentum coefficients became

$$\langle c_\mu \rangle \equiv \frac{2h}{c}\left(\frac{T_\infty}{T_j}\right)\frac{\langle u' \rangle^2}{U_\infty^2} \tag{15}$$

$$c_\mu \equiv \frac{2h}{c}\left(\frac{T_\infty}{T_j}\right)\frac{U_j^2}{U_\infty^2} \tag{16}$$

We assumed

$$T_j \equiv \frac{T_I + T_e}{2} \tag{17}$$

Figure 6 presents velocity profiles of u'_d measured about one slot width downstream of the slot exit. They are compared with a velocity profile of a steady wall-jet issuing from the slot. The primary difference between the fluctuating and steady jets is an increased spreading at the outer edge (i.e., away from the wall) of the oscillatory jet. This is expected because the suction part of the cycle resembles a sink flow rather than a jet. There is no evident effect of the level of the cavity pressure fluctuations on the shape of the oscillatory jet. The u'_d averaged over the core of the oscillatory wall-jets (shown in Fig. 6) is used for the slot calibration, as shown in Fig. 5. The estimation of u'^2_d for any given test condition in the cryogenic wind tunnel was extracted using the measured p'_I/ρ_{cryo}. Then u'^2_d was calculated for the same value of p'_I/ρ_{amb} using the polynomial fits to the ambient calibration data for that frequency, such as those presented in Fig. 5. The calculated u^2_d was introduced into either Eq. (14) or (15), depending on the level of steady blowing.

Because the characterization of the oscillatory blowing was performed with only a few steady blowing rates superimposed on the oscillations, it is desirable to know the effect of changing the mean mass flow rate on the estimation of u'_d. It was shown that the addition of steady blowing does not affect the relationship between u'_d and p'/ρ (Ref. 13). It was also demonstrated that the excitation is close to being two-dimensional.[13]

IV. Discussion

A. Control Applied from the LE Region

The pressure distribution of the NACA 0015 airfoil (Fig. 2a) at positive angles of attack contains a strong suction peak at the LE, followed by a steep adverse pressure gradient (pressure recovery) on the upper surface. At moderate and high Reynolds numbers, transition takes place very close to the LE. As α increases, the boundary layer over the airfoil upper surface thickens and tends to separate from the airfoil trailing edge (TE). This initial TE separation determines the airfoil $C_{l,\max}$. As α is further increased, the separation creeps toward the LE. Controlled cyclic excitation introduced from the LE region of different airfoils at low R_c (Refs. 7 and 9) delayed the boundary-layer separation and its propagation upstream, generating an increased $C_{l,\max}$, milder stall characteristics, and delaying drag divergence. The efficiency of the LE actuation is low (unless the attached region of the boundary layer amplifies the oscillations) because the separation starts at the TE and the control is applied at the LE. However, we began applying this kind of control because of the low R_c data available for comparison.

Figure 7 presents a comparison of lift data taken at $R_c = 37.6 \times 10^6$ and incompressible Mach numbers with data taken on a similar airfoil at $R_c = 0.9 \times 10^6$. The high R_c lift data were normalized by a single factor that matches the baseline $C_{l,\max}$ of the two data sets to account for wall interference and allow direct comparison of the lift increment because of the control. The comparison between the controlled data taken at the two R_c, using approximately the same mode of control (i.e., F^+ and C_μ), shows identical lift increments at poststall angles of attack, even though R_c was increased by a factor of 42. The $C_{l,\max}$ was increased by 12%, α of $C_{l,\max}$ was delayed by 2 deg, and stall was milder.

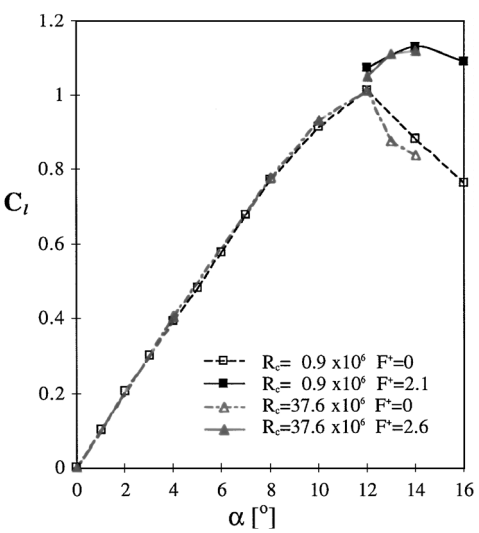

Fig. 7 Comparison of baseline (– – –) and controlled (——) data acquired at low ($R_c = 0.9 \times 10^6$, $M = 0.12$) and high ($R_c = 37.6 \times 10^6$, $M = 0.3$) R_c ($\delta_f = 0$ deg, LE slot used).

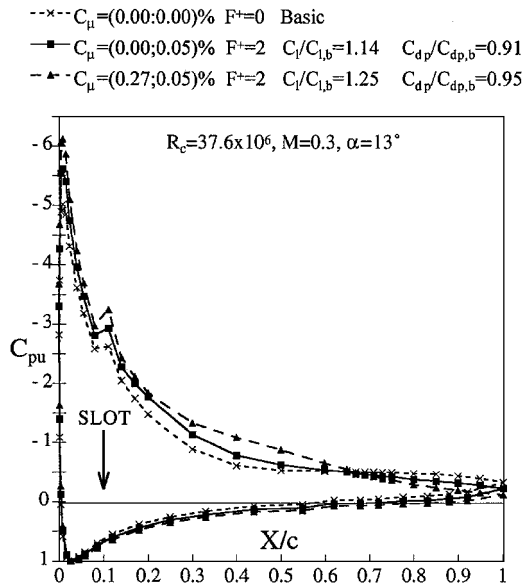

Fig. 8 Baseline and controlled pressure distributions showing the effect of added steady blowing ($\alpha = 13$ deg).

The data presented in Fig. 7 were repeated with $c_\mu = 0$ because in real applications it is desirable to use local actuators that do not rely on the supply of high-pressure gas via pipes or ducts while generating the sufficient control output (i.e., $\langle c_\mu \rangle$). Additionally, momentum efficiency considerations indicate that zero-mass-flux disturbances are more efficient for separation control. However, when performance and flexibility are of prime concern, the addition of weak steady blowing might prove beneficial. Figure 8 presents pressure distributions acquired while the airfoil was at $\alpha = 13$ deg. Separation takes place at $X/c \approx 0.4$, although the active slot is located at $X/c = 0.1$. At this incidence, the addition of $c_\mu = 0.27\%$ to the $\langle c_\mu \rangle = 0.05\%$ almost doubles the lift increment. As the incidence is increased[13] (to $\alpha = 14$ deg; data not shown) and the baseline separation moves closer to the active slot, it is sufficient to use oscillatory blowing with zero-mass-flux to obtain similar gains in performance. In the latter case, the efficiency of the imposed oscillations increases dramatically because the total momentum input (i.e., $c_\mu + \langle c_\mu \rangle$) is reduced by a factor of 6. Typically, the development of a separated flow region on the airfoil is accompanied by a rapid drag divergence. Under these conditions the momentum deficit decreases and the unsteadiness of the baseline wake is reduced as a result of the control applied near the LE.[13] Therefore one may conclude that the result of exciting the separating flow is not only to increase the lift, generate a milder stall, and delay the occurrence of drag divergence but also to reduce flow unsteadiness.

B. Control Applied over the Deflected Flap

It was shown previously[6,9] that the most efficient location for separation prevention is as close as possible to its inception, i.e., close to the TE. This is clearly the case when applying separation control to a flapped airfoil. It is well known that flap effectiveness decreases as the flap deflection angle increases, because of an increased adverse pressure gradient. For a fixed-flap deflection and increasing angle of attack, the flap effectiveness decreases also because of excessive boundary-layer growth upstream of the separation point. The complexity of modern high-lift systems stems partly from the need to reenergize the upper surface boundary layers, and the desire to achieve higher lift by simply increasing the wing area. Low R_c

tests demonstrated that oscillatory blowing is capable of delaying flow separation from a flap very effectively.[6,8] It allows buildup of increased suction over the entire upper surface of the airfoil, probably because it alters the direction of the streamline separating from the flap upper surface while eliminating the increased drag attributed to the widening wake. Delaying flow separation from the flap at elevated R_c is a vital step toward implementation of this technique.

The NACA 0015 airfoil was tested with the 30% chord flap deflected at an angle of 20 deg (Fig. 2b) to study the effect of elevated R_c on the performance of the flap separation control technique. Without control, the flap upper surface is separated at all α considered (see the plateau in the baseline pressure distributions in Fig. 9a for $X/c > 0.7$). Control was applied by introducing oscillatory blowing

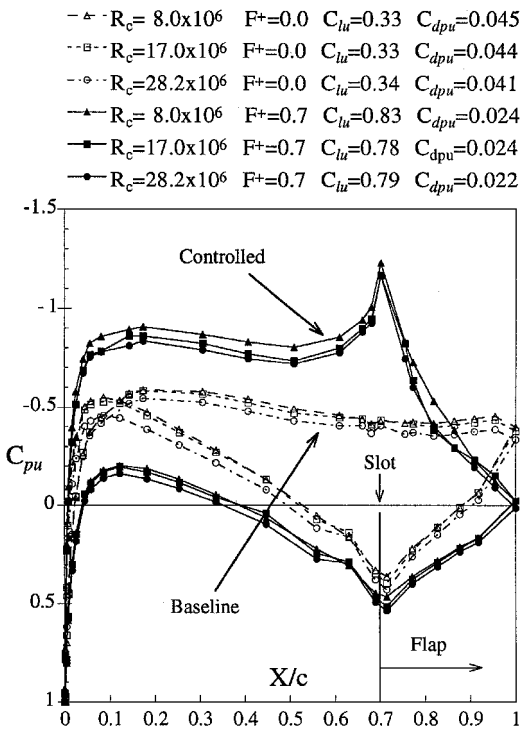

Fig. 9a Baseline and flap controlled pressure distributions; $M = 0.2$, $\alpha = -4$ deg, $X/c = 0.7$ slot used, $\delta_f = 20$ deg, and $c_\mu = (0.00;\ 0.05\%)$.

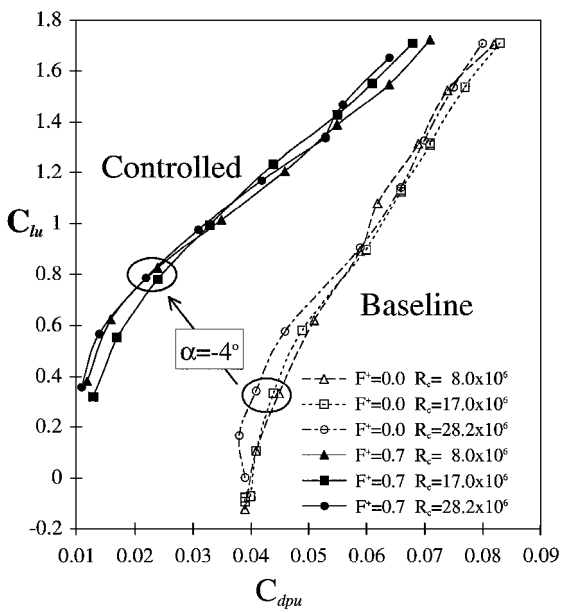

Fig. 9b Lift-form drag polars for the NACA 0015 airfoil with flap deflected and control applied at $X/c = 0.7$, $M = 0.2$, $\delta_f = 20$ deg, and $c_\mu = (0.00;\ 0.05\%)$.

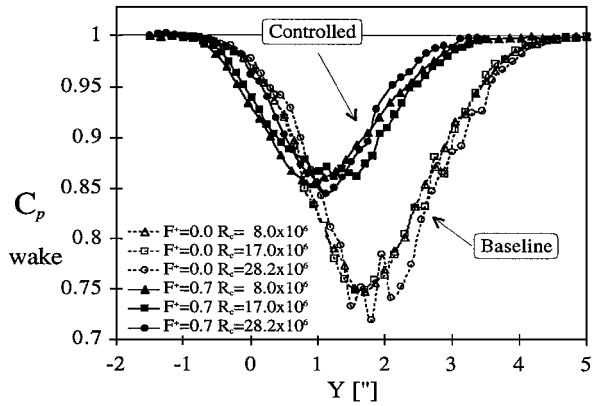

Fig. 9c Baseline and flap controlled wake surveys; $\alpha = -4$ deg, $M = 0.2$, $X/c = 0.7$ slot used, $\delta_f = 20$ deg, and $c_\mu = (0.00;\ 0.05\%)$.

from the slot located at the flap shoulder ($X/c = 0.7$, Fig. 2b). Zero-mass-flux disturbances were used (i.e., $c_\mu = 0$) to test the separation control technique when it is most efficient. The $F^+ = 0.7$ is well inside the range of the effective frequencies found in low R_c tests (Fig. 3; Ref. 9). Using oscillatory blowing, it was possible to reattach fully the flap flow at low angles of attack over the entire range of R_c (Fig. 9a). The C_{pTE} was increased from about -0.4 to 0, a high level of pressure recovery was restored over the flap, the circulation around the entire airfoil was increased, the lift was doubled, and the form-drag was reduced by 50% ($\alpha = -4$ deg; Fig. 9a).

Figure 9b presents the lift-form-drag polars of the baseline and controlled-flap airfoil at $R_c = 8.0$, 17.0, and 28.2×10^6. The form-drag is the main cause for the increased drag of separated flows. Presently, most of the drag is generated by the stalled flap. The excellent agreement between the three data sets (Fig. 9b) shows that the same F^+ and $\langle c_\mu \rangle$ are effective regardless of R_c. It can be seen that 50–75% of the form-drag was eliminated (at $C_l < 1$) because of maintenance of attached flow to the flap upper surface at low incidence (as shown in the pressure distributions presented in Fig. 9a) and smaller separated regions accompanied by narrower wakes, once separation could not be eliminated entirely at high α. The circles superimposed on Fig. 9b denote data acquired at $\alpha = -4$ deg showing the increase in lift and the reduction in form-drag. The reduced capability of the oscillatory blowing to maintain attached flow on the flap at high α results from it being tuned (in terms of $\langle c_\mu \rangle$) to restore attached flow at $\alpha = -4$ deg fully. This $\langle c_\mu \rangle$ is insufficient at increasing adverse pressure gradient over the flap and increased momentum loss of the upstream boundary layer, as α is increased (see also Fig. 9b in Ref. 8).

Figure 9c presents the wake rake data corresponding to the pressure distributions presented in Fig. 9a for $\alpha = -4$ deg. It shows very good agreement between the three data sets in terms of the wake shapes and resulting drag coefficients. The oscillatory excitation reduced the wake momentum deficit by 50% for a very wide range of R_c, indicative of the very weak R_c dependence of the separation control technique using oscillatory blowing.

The efficiency of oscillatory blowing for separation control can be appreciated when comparing the required momentum input for similar gains in airfoil performance using either oscillatory or steady blowing. Figure 10 presents the lift coefficient of the flapped NACA 0015 airfoil when the control was applied at the flap shoulder (Fig. 2b) and the airfoil was at $\alpha = -2$ deg. Oscillatory blowing with $\langle c_\mu \rangle = 0.03\%$ reattaches the flow to the flap and consequently almost doubles C_l. Note that the baseline lift is shown for $\langle c_\mu \rangle = 0.001\%$ because of the logarithmic scale used. The lift data for the steady blowing (Fig. 10) indicate that one would need to use two orders of magnitude larger steady blowing, $c_\mu = 2.7\%$, to gain the same lift increment. The two order-of-magnitude difference in effectiveness of oscillatory over steady blowing for separation control was observed for numerous geometries (LE application at poststall,[9] simple flap shoulder,[6] slotted flap,[9] swept airfoil,[14] flaps of finite wing planform[18]), and a range of R_c that varied by almost three orders of magnitude (6×10^4–4×10^7). The main source for the superior efficiency of oscillatory over steady blowing is the enhanced mixing

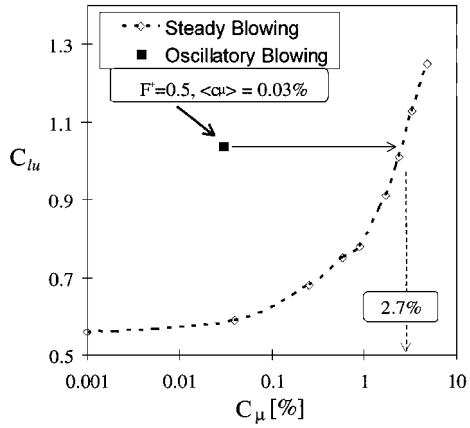

Fig. 10 Lift increment because of the use of oscillatory or steady flap blowing; $\alpha = -2$ deg, $M = 0.2$, $R_c = 17.0 \times 10^6$, and $\delta_f = 20$ deg.

across the boundary layer, promoted by the large periodic structures with predominant spanwise vorticity. These vortices remove the low momentum fluid from the vicinity of the surface and bring in high momentum flow from the freestream. Steady blowing creates a wall-jet that reenergizes the near-wall region of the boundary layer, but relies solely on its initial momentum because it does not mix with the external flow and suffers substantial viscous losses because of very high wall-shear.

The lift and drag polars presented in Figs. 11a and 11b show the relative effectiveness of the various frequencies used in the experiment, as well as the steady blowing used to reattach the flow to the flap upper surface. The data presented in these figures were acquired in the following manner: The airfoil was set at a negative α and the level of control input ($\langle c_\mu \rangle$ while maintaining $c_\mu = 0$, or c_μ while $\langle c_\mu \rangle = F^+ = 0$) was adjusted to obtain the same lift increment ($\Delta C_{lu} \approx 0.5$ at $\alpha = -4$ deg), regardless of F^+. Thereafter, α was increased and the nature of the flow separation was documented. The data presented in Figs. 11a and 11b were corrected for wind tunnel wall interference using the method presented in Ref. 19.

The reduced frequencies tested were $F^+ = 0.5$, 0.7, and 1.1, and all were effective. Lower values of F^+ are apparently more resistant to separation as α increases. They also require less momentum input when compared to the higher frequencies and are easier to generate. These F^+ are well inside the band of the effective frequencies found in low R_c tests (Ref. 9, Fig. 3). The lower frequencies are also more desirable because lower p' is required inside the airfoil cavity to generate the same $\langle c_\mu \rangle$. The $F^+ \approx 0.25$ was also tested but found to be ineffective. The lift-drag polars of Fig. 11b account for the added momentum (i.e., C_l vs $C_d + C_\mu$ was plotted rather than the drag alone). The baseline drag is high because of the flap separation at all α considered, whereas more than 50% of the drag was eliminated because of the delay of flow separation at low α, regardless of F^+. The efficiency of the zero-mass-flux oscillatory blowing is examined again by comparing it to steady blowing. Steady blowing with $c_\mu = 2.0\%$ generated the same C_l at low α (Fig. 11a) and lower total drag at higher α (Fig. 11b), but when the added momentum is taken into account it is clear that oscillatory blowing is more efficient by two orders of magnitude than steady blowing (Fig. 11b). Specifically, if the net efficiency of the added momentum is calculated in the form $(\Delta C_d - C_\mu)/C_\mu$, it is found that for oscillatory blowing it is $\mathcal{O}(100)$ whereas for steady blowing it is $\mathcal{O}(1)$.

C. Approaches for Closed-Loop Active Separation Control

Active flow control could prove beneficial when "natural" flow fails to maintain a desired pattern, and adverse effects limit the performance of flow-related machines. Such an adverse effect is flow separation under adverse pressure gradient. The optimal use of the separation control technology would be to incorporate it into an innovative design (such as 20%+ thick single element airfoils, rapidly converging aft fuselage, highly deflected nacelles, etc.). Such a design should contain an adverse pressure gradient, greater than the maximum possible at the design flow conditions (i.e., Reynolds and Mach numbers, boundary-layer characteristics at that location, and

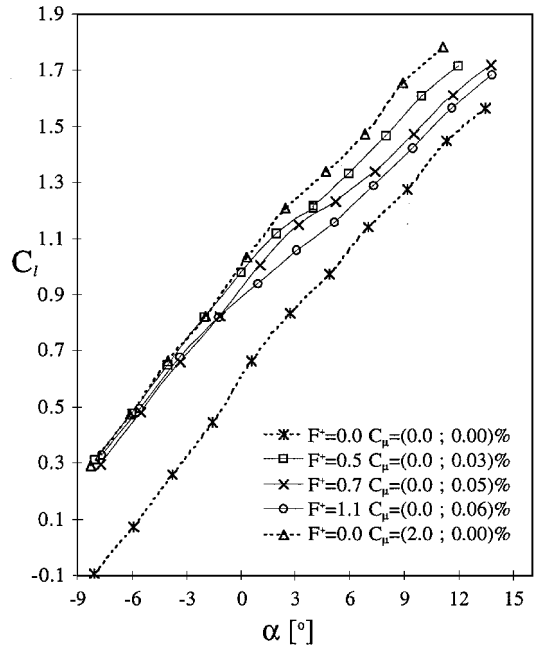

Fig. 11a Airfoil lift for different F^+ and steady flap blowing; $M = 0.2$, $R_c = 17.0 \times 10^6$, and $\delta_f = 20$ deg.

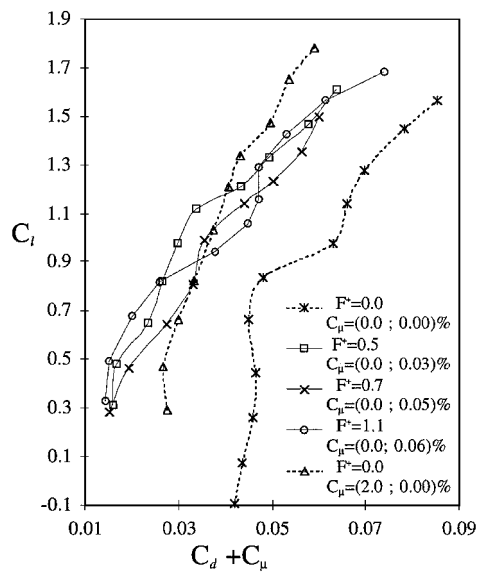

Fig. 11b Lift-drag polars (with C_μ taken into account). Same conditions as in Fig. 7a.

various geometrical constraints). Furthermore, the designer cannot assume that $\langle c_\mu \rangle$ greater than 0.1% could be generated, using conventional state-of-the-art technology, unless the flight speed would be extremely low (such as in micro-aerial-vehicles). One obvious measure of the success of a separation control technique is the maintenance of pressure recovery over the surface from which the flow tends to separate in the absence of control. Therefore the average pressure recovery over the controlled surface (i.e., over the flap starting at $X/c = 0.75$ to the TE) was calculated for the baseline, $F^+ = 0.5$, and for steady blowing with $c_\mu = 2\%$ (Fig. 12). The data presented in Fig. 12 show that in the baseline there is no pressure recovery over the flap, i.e., it is separated for all α. Applying oscillatory blowing with $\langle c_\mu \rangle = 0.03\%$ and $F^+ = 0.5$ at the flap shoulder generates a pressure recovery parameter of about 2–3 at $\alpha \leq -2$. As the α increases, both the adverse pressure gradient and the boundary-layer momentum loss increases; therefore the same $\langle c_\mu \rangle$ is incapable of producing the same benefits in performance. This is the reason why the pressure recovery decreases, indicating the development of separated flow. It is interesting to note that oscillatory blowing is more effective (at $\alpha < 2$ deg) than steady blowing with two orders

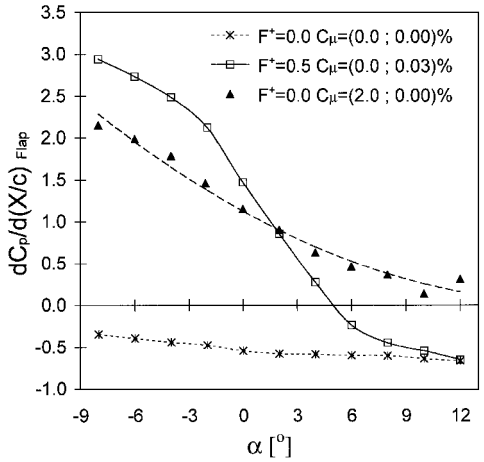

Fig. 12 Flap pressure recovery for oscillatory and steady flap blowing; $M = 0.2$, $R_c = 17.0 \times 10^6$, and $\delta_f = 20$ deg.

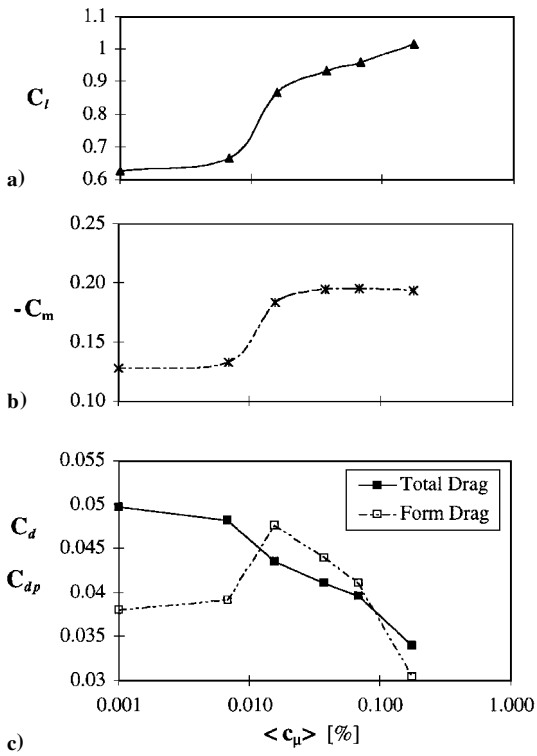

Fig. 13 Effect of increasing $\langle c_\mu \rangle$ applied at the flap shoulder on a) lift, b) moment, and c) drag coefficients; $\alpha = 0$ deg, $M = 0.2$, $R_c = 8.0 \times 10^6$, $\delta_f = 20$ deg, $F^+ = 0.7$, $c_\mu = 0$.

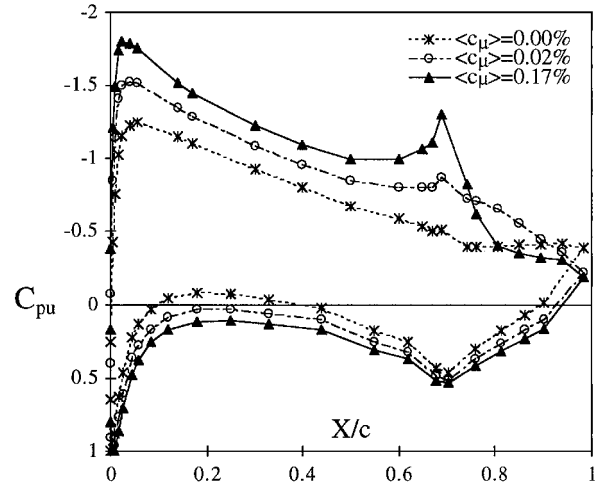

Fig. 14a C_p for different $\langle c_\mu \rangle$ applied at the flap shoulder ($\alpha = 0$ deg, $M = 0.2$, $R_c = 8.0 \times 10^6$, $\delta_f = 20$ deg, $F^+ = 0.7$, $c_\mu = 0$).

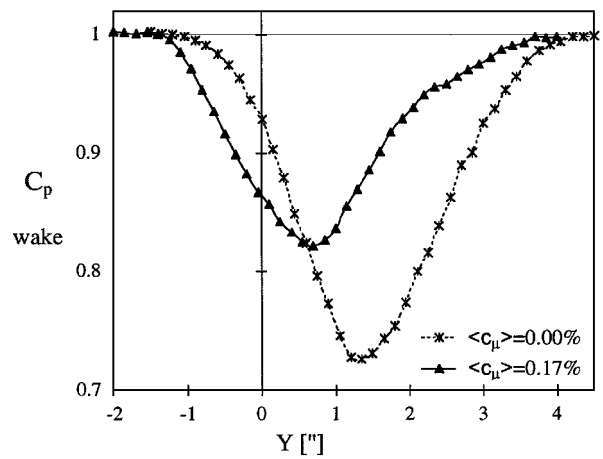

Fig. 14b Wake rake surveys for baseline and controlled flap ($\alpha = 0$ deg, $M = 0.2$, $R_c = 8.0 \times 10^6$, $\delta_f = 20$ deg, $F^+ = 0.7$, $c_\mu = 0$).

of magnitude greater momentum coefficient also in terms of these local parameters. The trailing edge pressure, which provides a very sensitive indication for the development of TE separation, shows similar trends as the pressure recovery parameter.[13]

These data could also give an indication of the expected performance benefits from applying separation control to an existing geometry: maintaining attached flow for $\Delta\alpha \approx 5$ deg beyond "natural" separation for the given flow conditions and geometry (similar to conventional control surfaces). The question of what is the allowable adverse pressure gradient while maintaining attached flow, for various other geometries remains. It is impractical to resolve this issue experimentally. Therefore there is a need for a prediction and design tool, benchmarked against a reliable existing data set.

Understanding the effect of $\langle c_\mu \rangle$ (i.e., the level of control input) is probably the most difficult of all the governing parameters. This is because of the nonlinear nature of the reattachment process and the significant hysteresis existing between the prevention of boundary-layer separation and the reattachment of separated flow.[8,20,21] However, it is crucial to understand this effect to develop a separation control strategy. In one possible control scheme, the frequency should scale according to $F^+ \approx 1$ (i.e., with the length of the potentially separated region and the freestream velocity) and the $\langle c_\mu \rangle$ should be modified to achieve the desired control output (one of the airfoil integral parameters such as C_l or C_m). Figures 13a–13c present the airfoil lift, moment, and drag data, respectively, as a function of the excitation level $\langle c_\mu \rangle$. Again, the baseline performance is shown for $\langle c_\mu \rangle = 0.001\%$. Figure 14a presents selected pressure distributions. The baseline flap is separated, as shown by the plateau in c_p for $X/c > 0.75$. When an $\langle c_\mu \rangle = 0.02\%$ was applied, it created a separation bubble above the deflected flap (Fig. 14a). This separation bubble increases the lift as well as the form-drag but causes an apparent reduction in the total drag (Fig. 13c). This apparent reduction in the total drag is probably erroneous, caused by the measurement technique combined with the flow unsteadiness. Once the level of control input is increased to an $\langle c_\mu \rangle = 0.17\%$, the separation bubble is eliminated (Fig. 14a), causing a reduction in both the form and total drag, and a further increase in the lift (Fig. 13a). Once the form-drag is lower than the total drag and there is no indication of significant unsteadiness over the airfoil that might shed vortices into the wake, it is safe to calculate the wake deficit from the wake surveys (presented in Fig. 14b) and assume it is the drag. Even when using an $\langle c_\mu \rangle = 0.17\%$, the drag reduction is still an order of magnitude greater than the excitation momentum input. The airfoil moment coefficient about the quarter chord (Fig. 13b) behaves in a similar manner to the lift when the $\langle c_\mu \rangle$ is increased,

but saturates earlier, whereas the C_l continues to increase slowly (Fig. 13a, $\langle c_\mu \rangle > 0.02\%$).

In terms of control strategy, if one would like to restore and maintain a certain level of pressure recovery on the flap, it is possible to use C_{pTE} as a single control input in a control system.[13] A sensor for steady TE pressure would suffice, or perhaps two sensors—one on the mid-chord of the flap and the second at the TE to measure the flap pressure recovery—while $\langle c_\mu \rangle$ (as indicated by the oscillating cavity pressure) is suitable as an actuator output. The $F^+ \approx 1$ could be maintained at all times.

V. Conclusions

Active separation control was applied successfully for the first time at Reynolds numbers corresponding to a jetliner at takeoff conditions. Oscillatory blowing proved to be an effective and efficient tool for the control of boundary-layer separation over a wide range of chord Reynolds numbers, representative of a micro-aerial-vehicle to a commercial jetliners at takeoff. It was demonstrated that the frequency of oscillations should be chosen such that $0.5 < F^+ < 1.5$ regardless of the Reynolds number.

Using bench-top experiments, accompanied by theoretical analysis, it was determined that the level of velocity fluctuations exiting the blowing slot (u') is proportional to the cavity pressure fluctuations normalized by the density p'/ρ, for low amplitudes ($u' < 10$ m/s), whereas for high amplitudes it is proportional to $\sqrt{(p'/\rho)}$. This parameter was used to correlate the ambient bench-top experiment with the cryogenic wind tunnel experiment and estimate the oscillatory blowing momentum coefficients used in the cryogenic wind tunnel experiment, where such measurement is impractical. A possible approach to closed-loop control of separation is to sense the TE pressure and use it as an input while adjusting $\langle c_\mu \rangle$ to achieve the desired aerodynamic behavior while maintaining $F^+ \approx 1$ at all times.

The result of introducing controlled excitation into a separating flow over an airfoil (and other geometries) is not only to increase the lift and reduce the drag but also to reduce flow unsteadiness on the body and in its wake. Unsteady separation control could be used to simplify and reduce the weight of high-lift systems. Although the experiments focused on airfoils, the same approach could be used to delay flow separation and overcome steeper adverse pressure gradients in diffusers, inlets, jet nozzles, and aft fuselages. It could increase the efficiency of conventional control surfaces, decrease their size, allow quicker handling of gusty conditions, and backup or even replace conventional control strategies. However, these benefits cannot be realized without further development of prediction and design tools as well as suitable actuators.

Acknowledgments

This work was performed while the first author held a National Research Council–NASA Langley Research Center research associateship. The authors would like to thank R. W. Wlezien and I. Wygnanski for the special efforts undertaken to make this experiment possible. The authors would also like to thank W. L. Sellers III, C. B. McGinley, B. K. Stewart, and the entire 0.3mTCT crew from LaRC for their support and J. T. Lachowicz for reviewing the manuscript.

References

[1]Gad-el-Hak, M., and Bushnell, D. M., "Separation Control: Review," *Journal of Fluids Engineering*, Vol. 113, March 1991, pp. 5–30.

[2]Neuburger, D., and Wygnanski, I., "The Use of a Vibrating Ribbon to Delay Separation on Two Dimensional Airfoils: Some Preliminary Observations," *Proceedings of the Workshop II on Unsteady Separated Flow*, edited by J. M. Walker, Frank J. Seiler Research Lab., U.S. Air Force System Command, Colorado Springs, CO, 1988, pp. 333–341.

[3]Bar-Sever, A., "Separation Control on an Airfoil by Periodic Forcing," *AIAA Journal*, Vol. 27, No. 6, 1989, pp. 820–821.

[4]Collins, F. G., "Boundary-Layer Control on Wings Using Sound and Leading Edge Serrations," AIAA Paper 79-1875, Aug. 1979.

[5]Williams, D., Acharya, M., and Yang, B. P., "The Mechanism of Flow Control on a Cylinder with the Unsteady Bleed Technique," AIAA Paper 91-0039, Jan. 1991.

[6]Seifert, A., Bachar, T., Koss, D., Shepshelovich, M., and Wygnanski, I., "Oscillatory Blowing, a Tool to Delay Boundary-Layer Separation," *AIAA Journal*, Vol. 31, No. 11, 1993, pp. 2052–2060.

[7]Seifert, A., Darabi, A., Nishri, B., and Wygnanski, I., "The Effects of Forced Oscillations on the Performance of Airfoils," AIAA Paper 93-3264, July 1993.

[8]Nishri, B., "On the Dominant Mechanisms Governing Active Control of Separation," Ph.D. Dissertation, Dept. of Fluid Mechanics and Heat Transfer, Tel-Aviv Univ., Tel-Aviv, Israel, 1995 (in Hebrew).

[9]Seifert, A., Darabi, A., and Wygnanski, I., "On the Delay of Airfoil Stall by Periodic Excitation," *Journal of Aircraft*, Vol. 33, No. 4 , 1996, pp. 691–699.

[10]Wygnanski, I., Oster, D., and Fiedler, H., "A Forced, Plane, Turbulent Mixing-Layer: A Challenge for the Predictor," *Turbulent Shear Flows 2*, edited by L. J. S. Bradbury, F. Durst, B. E. Launder, F. W. Schmidt, and J. H. Whitelaw, Springer–Verlag, New York, 1980, pp. 314–326.

[11]Collins, F. G., and Zelenevitz, J., "Influence of Sound upon Separated Flow over Wings," *AIAA Journal*, Vol. 13, No. 3, 1975, pp. 408–410.

[12]Sigurdson, L. W., and Roshko, A., "Controlled Unsteady Excitation of a Reattaching Flow," AIAA Paper 85-0552, March 1985.

[13]Seifert, A., and Pack, L. G., "Oscillatory Control of Separation at High Reynolds Numbers," AIAA Paper 0214-98, Jan. 1998.

[14]Naveh, T., Seifert, A., Tumin, A., and Wygnanski, I., "The Effect of Sweep on the Parameters Governing the Control of Separation by Periodic Excitation," *Journal of Aircraft*, Vol. 35, No. 3, 1997, pp. 510–512.

[15]Hites, M., Nagib, H., Seifert, A., Wygnanski, I., Darabi, A., and Bachar, T., "Airfoil Lift Enhancement Through Oscillatory Blowing," 48th American Physical Society/Div. of Fluid Dynamics Meeting, Irvine, CA, Nov. 1995.

[16]Rallo, R. A., Dress, D. A., and Siegle, H. J. A., "Operating Envelope Charts for the Langley 0.3-Meter Transonic Cryogenic Wind Tunnel," NASA TM-89008, 1986.

[17]Ladson, C. A., and Ray, E. J., "Evolution, Calibration, and Operational Characteristics of the Two-Dimensional Test Section of the Langley 0.3-Meter Transonic Cryogenic Tunnel," NASA TP-2749, 1987.

[18]Seifert, A., Bachar, T., Wygnanski, I., Kariv, A., Cohen, H., and Yoeli, R., "Application of Active Separation Control to a Small Unmanned Air Vehicle," *Journal of Aircraft*, Vol. 36, No. 2, 1999, pp. 474–477.

[19]Rae, W. H., Jr., and Pope, A., *Low Speed Wind Tunnel Testing*, 2nd ed., Wiley, New York, 1984, pp. 349–361.

[20]Chang, P. K., *Separation of Flow*, Pergamon, Oxford, 1970.

[21]Nishri, B., and Wygnanski, I., "Effects of Periodic Excitation on Turbulent Flow Separation from a Flap," *AIAA Journal*, Vol. 36, No. 4, 1998, pp. 547–556.

M. Samimy
Associate Editor